B. Slavin, S. Levitan, and G. Buxton, "Mechanical modeling of failure in surface coatings," in proc. *SPIE Intl. Symp. on Smart Structures & Materials/NDE,* paper 5757-52, San Diego, California, March 2005.

Mechanical modeling of failure in surface coatings

Benjamin A. Slavin[a], Steven P. Levitan[a], Gavin A. Buxton[b]

[a]Department of Electrical and Computer Engineering, University of Pittsburgh;
[b]Department of Chemical and Petroleum Engineering, University of Pittsburgh

ABSTRACT

We present a computer model which allows us to explore the failure behavior of surface coatings. We use a quasi-static three-dimensional Lattice Spring Model coupled with the velocity Verlet algorithm to simulate surface coating on substrate systems. Fracture, elastic response, and shrinking are considered in our simulation method. The results provide a framework upon which the failure mechanisms of surface coatings can be investigated.

Keywords: Surface Coatings, Surface Failure, Simulation, Lattice Spring Model

1. INTRODUCTION

Films and surface coatings provide protection for the surfaces which they cover. This results in a longer lifespan for the underlying structures and, in turn, decreases the need for repairs or replacement.[1] These protective layers are subject to failure, and, upon failing, can lead to 'catastrophic degradation' of the structure which they protect. By increasing the longevity of surface coatings, it should be possible to increase the lifespan of these structures. We present a computer model which allows us to explore the failure of these materials.

Our approach models the failure of surface coatings through the use of the Lattice Spring Model (LSM) coupled with the velocity Verlet algorithm.[2,3] We utilize the internal strain created by environmental conditions as a basis for deformation as well as crack formation and propagation.

We continue by presenting related work, and describing the model. Following this, our simulation technique is discussed in detail. Finally, we discuss our results and conclusions, and provide an overview of our intended future work.

2. RELATED WORK

Prior research into modeling the failure of paint and other surface coatings has been limited in scope, and has often been dedicated to the modeling of this phenomenon for computer graphics purposes.[4,5,6] As such, researchers have typically been interested in producing results which are aesthetically appealing rather than results which are based on a chemical model.

More than this, the models which have been used tend to represent the surface as a single 2-dimensional layer. Hirota specifically points-out that the "[surface-only model] has the drawback that it is not applicable to the simulation of destruction" when compared to a three-dimensional model.[6]

Through the work of Buxton and Balazs, the Lattice Spring Model has been shown to be applicable to the simulation of polymer systems.[2] We use this model as the basis for our work.

[b]Dr. Gavin Buxton can be contacted at the Department of Chemistry, University of Durham

3. MODELING METHOD

The Lattice Spring Model has been shown to model the micromechanical behavior of highly heterogeneous polymer systems. It allows for the simulation of such systems through a representation of nodes connected by harmonic elements (also called springs or bonds). Figure (1) shows a two-dimensional LSM lattice. The black dots represent nodes, while the spring elements which connect them represent bonds. This lattice exhibits periodic boundary conditions; that is, the lattice is constructed in a manner such that it contains no edges. The dashed lines on the left-hand side of the figure represent the same bonds as those on the right-hand side. The same is true for the bonds on the top and bottom of the lattice.

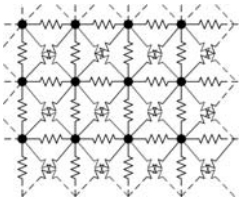

Figure 1. Two-dimensional LSM lattice with periodic boundary conditions

LSM accounts for the nearest and next-nearest neighbor interactions between nodes, resulting from bonds to the six orthogonal and twelve diagonal neighbors of a node. Figure (2) shows an individual node from a three-dimensional system. The sphere at the center represents the node, while the solid black lines represent the eighteen bonds which belong to the node. The dotted lines are provided for reference.

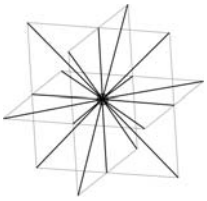

Figure 2. Single node from a three-dimensional LSM system; six orthogonal and twelve diagonal bonds can be seen

These nodes, when connected by bonds, form a mesh which represents a solid; in our case, a surface coating. Figure (3a) shows how LSM nodes are connected to form a mesh. Figure (3b) shows how LSM nodes can be mapped to a solid. For clarity, only the outer nodes are shown.

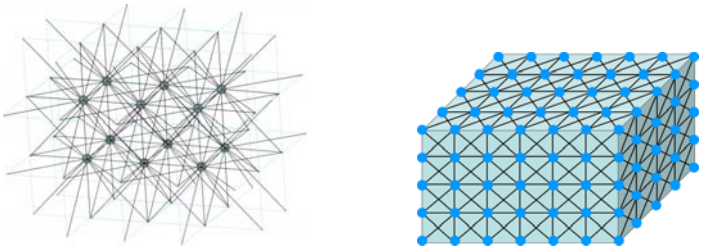

(a) (b)

Figure 3. LSM Mesh – (a) Three-dimensional LSM mesh of dimension 3x2x2; (b) Outer nodes in mapping of an LSM mesh to a solid

The LSM allows for the use of static, quasistatic,[3] and dynamic modeling methods. The use of a quasistatic approach for our model has resulted in a simulation which is less computationally intensive than a corresponding

dynamic model. We now discuss our simulation technique.

4. SIMULATION TECHNIQUE

The simulation technique which we have employed is based upon three primary phases; initialization followed by a macroscale and a microscale iterative process, as shown in Figure (4).

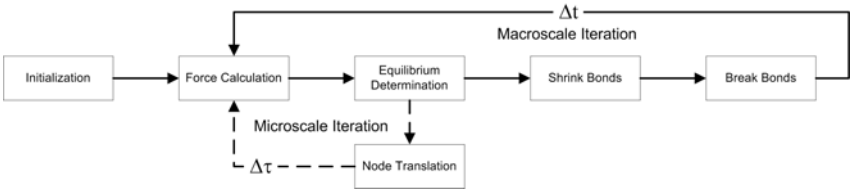

Figure 4.

During initialization, the LSM array is established and configured. It is populated with nodes which are subsequently assigned their location information (absolute spatial position). Each node is then marked with node-type information, indicating whether it is a coating node or a substrate node. Bonds between each node and its nearest and next-nearest neighbors are created using periodic boundary conditions in the directions parallel to the substrate. The natural length of each bond is set during initialization to be equal to the distance between the nodes which it connects. This natural length is not constant, and is changed during simulation to reflect contraction of the system.

The macroscale time steps encompass major changes which are made to the system. During the macroscale cycle, the system is first allowed to come to equilibrium through a varying number of microscale iterations. After reaching equilibrium, the system undergoes a contraction phase realized by a reduction in the natural length of the bonds. The final task in each macroscale iteration is the creation of fractures through analysis of the strain profile and the breaking of bonds. We now discuss each step in detail.

4.1. Microscale Iteration Loop

In each microscale iteration, the system is allowed to move toward equilibrium. This process is achieved by solving the velocity Verlet algorithm (Equations 4 through 7 below) for each node. Each iteration brings the system closer to equilibrium and will proceed to the next iteration until a minimum threshold is met, at which time control is returned to the macroscale loop.

4.1.1. Force Calculation

In the LSM, strain on a node is the vector sum of the strain on each of its bonds. In our current implementation, strain accounts for the only internal force within the system, and as such, the net force on a node is equal to the net strain on its bonds. Thus, the strain on a node i is a function of the forces imparted upon it by each of its j neighbors.

$$\vec{F}_i = \sum_{j=0} \vec{F}_{ij} \tag{1}$$

Each bond has an associated natural length, $\ell_{ij}(t)$, which is set during initialization and varies as the system contracts. The force asserted by a bond at a given time is proportional to the deviation of the bond length from this natural length, and is calculated from a modified Hooke's Law expression. The bond length is merely the vector distance, $\vec{R}_{ij}$, between the nodes which a bond connects. The spring constant for a bond, k_{ij} is determined by the properties of the surface coating being modeled.

$$\vec{F}_{ij} = -k_{ij} \cdot \frac{|R_{ij}| - \ell_{ij}}{|R_{ij}|} \cdot \vec{R}_{ij} \tag{2}$$

4.1.2. Equilibrium Determination

Once the net strain on all nodes has been calculated, the sum of the squared forces is compared to a threshold value.

$$\sum_{i=0} F_i^2 < \theta_{eq} \tag{3}$$

If the system meets the test condition, it is considered to be at equilibrium and we can stop the microscale iteration. Otherwise, the nodes must be allowed to move toward equilibrium.

4.1.3. Node Translation

For node translation, we have chosen to employ the velocity Verlet algorithm. A derivation of the Verlet algorithm, it allows the approximation of position ($\vec{R}$), velocity ($\vec{V}$), and acceleration ($\vec{A}$) after a time interval ($\Delta\tau$) based upon information of the same values immediately prior to the interval (time τ).[7,8] Damping is achieved through the use of a Stokes drag term (Θ), preventing unbounded oscillation.

$$\vec{R}_i(\tau + \Delta\tau) = \vec{R}_i(\tau) + \vec{V}_i(\tau) \cdot \Delta\tau + \tfrac{1}{2} \cdot \vec{A}_i(\tau) \cdot (\Delta\tau)^2 \tag{4}$$

$$\vec{V}_i\left(\tau + \tfrac{\Delta\tau}{2}\right) = \vec{V}_i(\tau) + \tfrac{1}{2} \cdot \vec{A}_i(\tau) \cdot \Delta\tau \tag{5}$$

$$\vec{A}_i(\tau + \Delta\tau) = \frac{-\vec{F}_i(\tau)}{m} - \Theta \cdot \vec{V}_i\left(\tau + \tfrac{\Delta\tau}{2}\right) \tag{6}$$

$$\vec{V}_i(\tau + \Delta\tau) = \vec{V}_i\left(\tau + \tfrac{\Delta\tau}{2}\right) + \tfrac{1}{2} \cdot \vec{A}_i(\tau + \Delta\tau) \cdot \Delta\tau \tag{7}$$

Once we have updated these values for all nodes, we begin the next microscale iteration, beginning with the calculation of force. During each macroscale iteration, there is a variable number of microscale iterations to reach equilibrium.

4.2. Bond Shrinking

Surface failure and fracture are due to the strain within a material or the substrate interface layer. Once equilibrium has been reached for the current bond lengths, we can proceed to model the shrinking of bond length due to environmental conditions. To simulate this phenomenon, we chose to decrease the natural length of the springs within the LSM over time. We assume that each bond has an original natural length (ℓ_0) and that, over time, it approaches a final, contracted, natural length (ℓ_f).

$$\ell_{ij}(t) = \ell_f + (\ell_0 - \ell_f) \cdot e^{-t \cdot \alpha_{ij}} \tag{8}$$

Strain can be induced as a result of environmental processes during the surface coating's lifespan. As such, we have chosen to simulate this by varying the amount of contraction by layer. Because the top layer is most exposed, it will be subject to the most rapid rate of contraction. Similarly, because the substrate interface layer is the least exposed, it will be subject to the most gradual rate of contraction.

This contraction must take place within the bonds that connect nodes. Because a bond connects two nodes which may be on different layers, we take the average of the contraction rates associated with each of the nodes.

$$\alpha_{ij} = \frac{\alpha_i + \alpha_j}{2} \tag{9}$$

The contraction rate α_n for a given node n is determined by a linear relationship based upon a node's vertical position, or Z-Index (zi_n), within the surface coating. The number of layers within the surface coating represents the height h of the lattice.

$$\alpha_n = \frac{zi_n}{h} \cdot \alpha_{top} + \frac{h - zi_n}{h} \cdot \alpha_{bottom} \tag{10}$$

4.3. Breaking Bonds

The breaking of bonds within the LSM system represents crack formation. We assume that crack formation, either within the surface coating itself or between the coating and a substrate, is the primary cause of failure for surface coatings.

Cracks form at areas of high strain; however, it is important to note that a crack may not always form at the area of highest strain. We have assumed that a minimum threshold must be met for a bond to break and that *any* bond which exceeds this threshold has an associated probability of breaking at a point in time.

We assume that the non-proportional probability of a bond breaking p_i is non-linear with respect to strain. This non-linearity is achieved by the use of an exponential constant (μ_k).

$$p_i(t) = \begin{cases} \frac{\vec{R}_{ij}(t)}{\ell_{ij}(t)} > \theta : \left(\frac{\vec{R}_{ij}(t)}{\ell_{ij}(t)} - \theta\right)^{\mu_k} \\ \frac{\vec{R}_{ij}(t)}{\ell_{ij}(t)} \leq \theta : 0 \end{cases} \tag{11}$$

The probability of a bond breaking P_i is normalized over the sum of all candidate bonds. Based upon these normalized probabilities, a bond is selected to be broken at random. That is, the likelihood of a bond being randomly selected is proportional to it probability of breaking.

$$P_i(t) = \frac{p_i(t)}{\sum_{j=0} p_j(t)} \tag{12}$$

In the event that no bond exceeds the threshold for breaking, no bonds will be broken. If at least one bond exceeds the threshold, one bond will be broken. Because we are using a quasistatic modeling method, we break only one bond at a time so that the change in the strain profile due to the breaking of a bond can be used in the determination of which bond should be broken next.

Following the breaking process, we advance the simulation to the next macroscale iteration. This process is repeated until a prescribed number of macroscale iterations have been completed.

5. RESULTS

5.1. Forced Cut

We first ran a series of tests to ensure that the simulation produced expected results under controlled conditions. These tests included first making a single cut in the surface coating and second making intersecting diagonal cuts and observing the response of the system based upon each. The third test we ran involved the cutting of a 'tongue' or 'slab' from the surface coating. The results of the simulation in which the tongue was cut are provided in Figure (5). This simulation included 2,000 nodes and took 2 macroscale and 4700 microscale iterations to generate the response seen in Figure (5b). Only 2 macroscale iterations were needed because no additional bonds were broken, and the system was able to reach equilibrium through the microscale iterative process.

The surface coating was cut from its surface down to the substrate on three sides of a square placed about its center. The slab which it formed was also detached from the substrate, leaving it connected on only one side (upper-right side of surface in Figure (5a)).

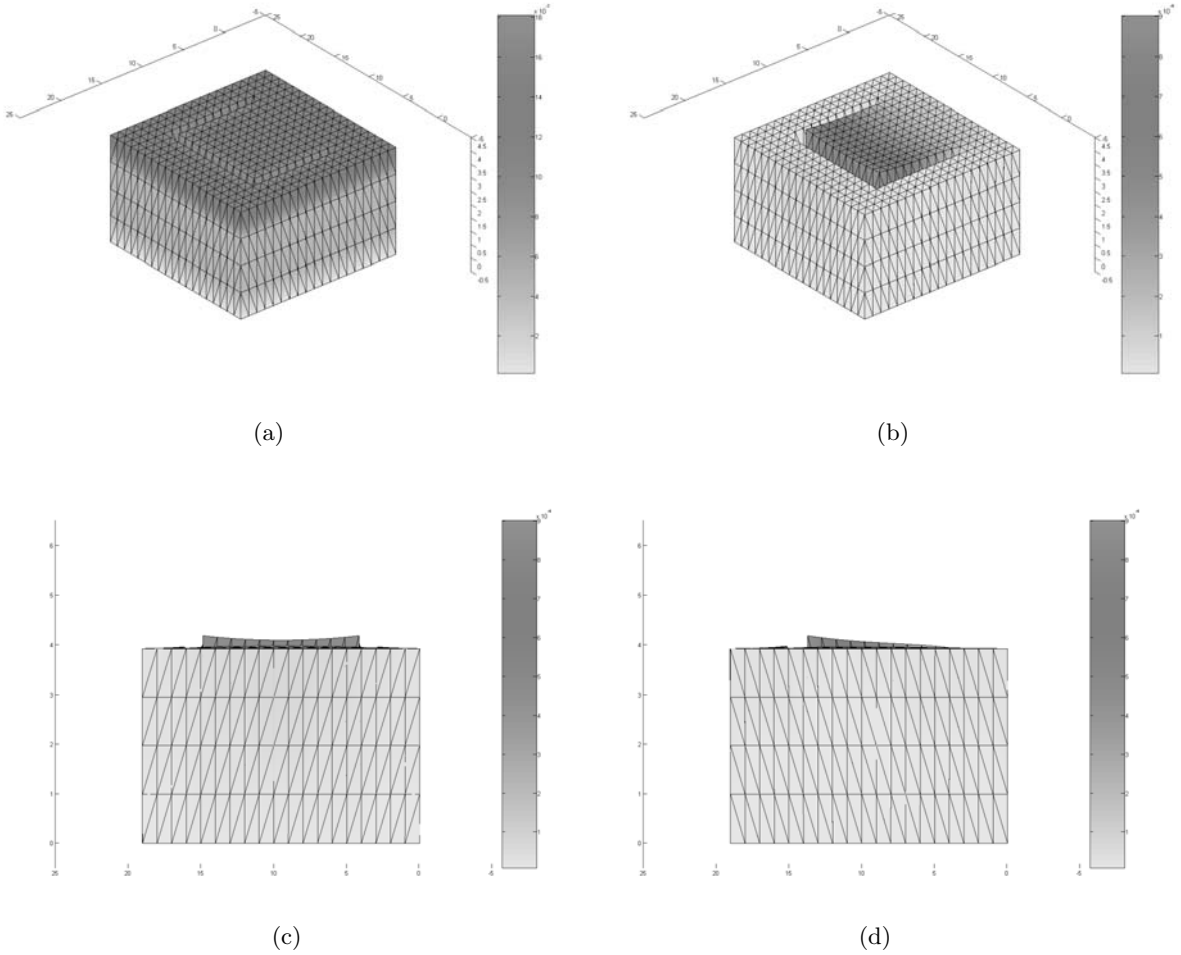

Figure 5. Forced cut, 'Tongue' configuration – (a) Surface prior to simulation; (b) Surface after simulation; (c) Surface after simulation as viewed from front; (d) Surface after simulation as viewed from near side

The simulation was run without the addition of bond breaking beyond those bonds which were explicitly cut to form the tongue. Periodic boundary conditions were maintained along the edges perpendicular to the substrate.

The results of this simulation show the contraction and curling of the surface coating as was expected given the model. High stress can be observed at the tip of the tongue as it tries to pull away from the substrate (5b, 5d). The tongue can also be observed to curl inward upon itself, due to strain on the surface layer (5c). Additionally, a response can be seen from the solid opposite the tongue in (5c) and (5d), as the solid tries to curl away from the cut in response to the formation of an edge.

5.2. Full Simulation

The simulation which generated the images of Figure (6) consisted of 8,000 nodes connected by 65,600 bonds, and is the result of 4,974 macroscale iterations. As in the case of the previous simulation, periodic boundary conditions were employed. Unlike the images from Figure (5), the varying coloration does not represent strain within the system.

As can be seen between Figure (6a) and Figure (6b), the system first experienced vertical contraction. This is the result of the bond-length contraction coupled with periodic boundary conditions. The vertical direction is

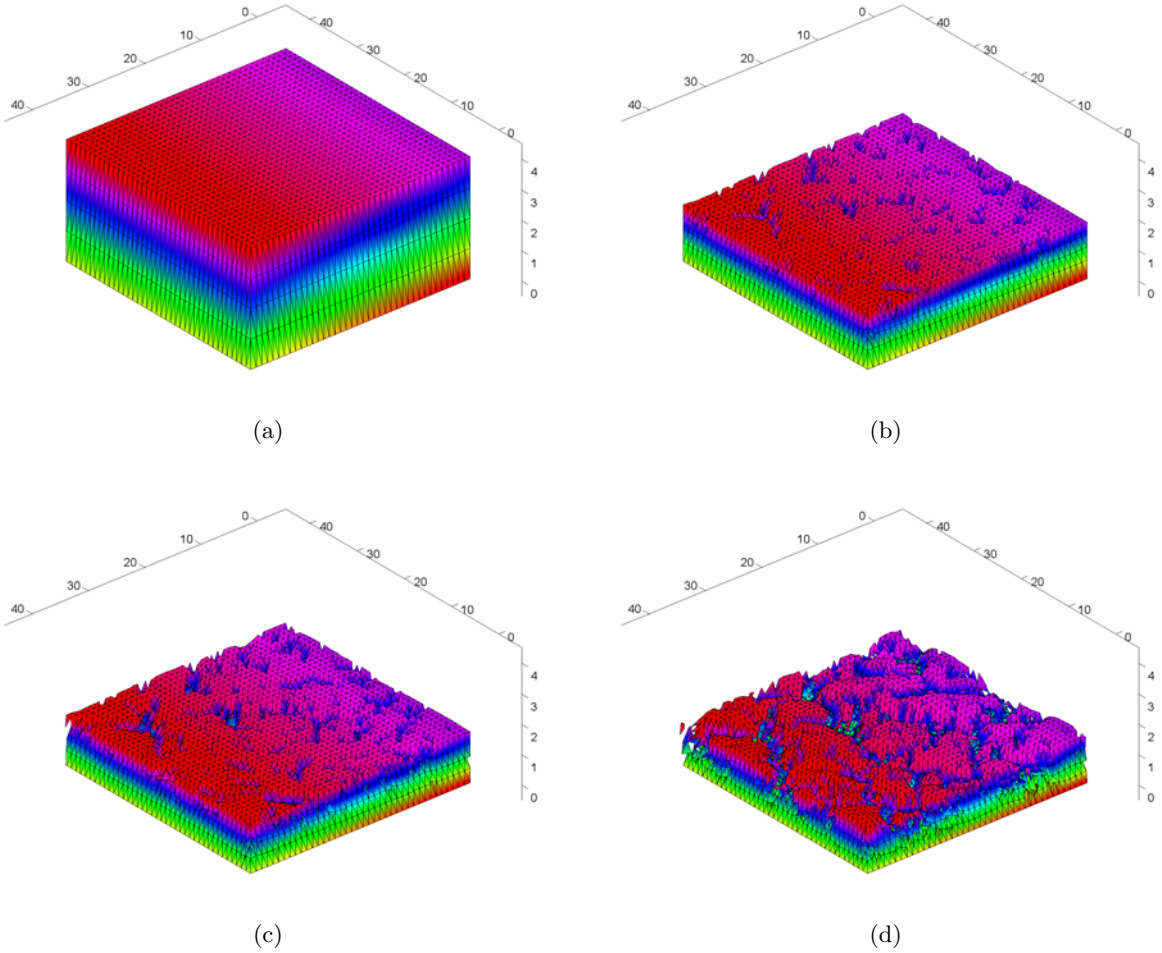

Figure 6. Full Simulation – (a) Surface prior to simulation; (b) Surface after 774 macroscale iterations; (c) Surface after 1574 macroscale iterations; (d) Surface after 4974 macroscale iterations

the only one which is not fully constrained and, as such, is the only direction in which the surface coating is free to move.

The cracks which appear in Figure (6b) are primarily on the exposed surface. This is due to the greater rate of contraction and the higher level of strain which it induces. Figure (6c) shows the lengthening of the cracks seen in Figure (6b) and the addition of a small number of new cracks. Cracks can also be seen to have increased in depth when compared to those in Figure (6b). A continued lengthening of cracks and depth increase can be seen in Figure (6d). Additionally, it is possible to observe the intersection of independently formed cracks.

At present, no peeling can be observed. This is because we have not yet implemented a weak surface coating-substrate interface adhesion. As such, delamination is not an expected outcome.

6. SUMMARY AND CONCLUSIONS

We have shown that the Lattice Spring Model is applicable for the construction of a three-dimensional model of surface coatings. Through our application of this model, we have shown that it is possible to simulate crack propagation with the LSM. Moreover, we have shown that it is possible to simulate multiple independent cracks within a solid with propagation of each occurring independently. Given this, we have shown that the simulation is consistent with our expectations of the model.

We have shown that the velocity Verlet algorithm is capable of generating useful results with reasonable simulation time when coupled with the Lattice Spring Model. The results shown in Figure (5) were generated over a period of approximately twenty minutes on a single 2.53GHz Pentium 4 workstation; however, approximately 95% of this time was spent generating and writing visualization data for animation. The results shown in Figure (6) were generated over a period of eight hours on a single 2.79GHz Pentium 4 workstation.

7. FUTURE WORK

We are currently calibrating our model with experimental data on paint. By doing this, we hope to more accurately simulate the properties of physical surface coatings. After calibrating our model with experimental data we will be able to simulate fracture for surface coatings with different intrinsic properties. In doing so, we intend to study and attempt to determine properties that control the failure rate for different coating types. From this data, we will endeavor to propose mechanisms to help prolong the lifespan of surface coatings.

Upon the realization of a sufficiently detailed model of surface coating failure, we also plan to investigate the behavior of self-healing surface coatings. Various methods of self-healing have been proposed, and we expect to explore the results which are due to these various processes.[9,10]

8. ACKNOWLEDGEMENTS

This work was supported by a grant from the Mascaro Sustainability Initiative at the University of Pittsburgh. The authors would like to thank Dr. Anna C. Balazs and José A. Martínez of the University of Pittsburgh as well as Dr. Peter Kamarchik of PPG Industries for their contributions.

REFERENCES

1. J. Huber, "Why is my paint peeling." Retrieved May 10, 2004 from http://www.thisoldhouse.com.
2. G. Buxton and A. C. Balazs, "Simulating the morphology and mechanical properties of filled diblock copolymers," *Physical Review W* **67**, p. 031802, 2003.
3. G. Buxton and A. C. Balazs, "Modeling the dynamic fracture of polymer blends processed under shear," *Physical Review B* **69**, p. 054101, 2004.
4. E. Paquette, P. Poulin, and G. Drettakis, "The simulation of paint cracking and peeling," in *Graphics Interface 2002 Conference Proceedings*, pp. 59–68, 2002.
5. S. Gobron and N. Chiba, "Crack pattern simulation based on 3d surface cellular automata," *The Visual Computer* **17**, pp. 287–309, 2001.
6. K. Hirota, Y. Tanoue, and T. Kaneko, "Generation of crack patterns with a physical model.," *The Visual Computer* **14**(3), pp. 126–137, 1998.
7. L. Verlet, "Computer 'experiments' on classical fluids. i. thermodynamical properties of lennard-jones molecules," *Physical Review* **159**, pp. 98–103, 1967.
8. L. Verlet, "Computer 'experiments' on classical fluids. ii. equilibrium correlation functions," *Physical Review* **165**, pp. 201–214, 1968.
9. S. R. White, N. R. Sottos, P. H. Geubelle, J. S. Moore, M. R. Kessler, S. R. Sriram, E. N. Brown, and S. Viswanathan, "Autonomic healing of polymer composites," *Nature* **409**, pp. 794–797, 2001.
10. X. Chen, M. Dam, K. Ono, A. Mal, H. Shen, S. Nutt, K. Sheran, and F. Wudl, "A thermally re-mendable cross-linked polymeric material," *Science* **295**, pp. 1698–1702, 2002.